HHS Public Access

Author manuscript

J Immunol. Author manuscript; available in PMC 2018 June 01.

Published in final edited form as:

J Immunol. 2017 June 01; 198(11): 4293–4303. doi:10.4049/jimmunol.1700261.

Bacterial Siderophores Hijack Neutrophil Functions

Piu Saha[*,‖], **Beng San Yeoh**[*,‖], **Rodrigo A. Olvera**[*], **Xia Xiao**[*], **Vishal Singh**[*], **Deepika Awasthi**[†], **Bhagawat C. Subramanian**[‡], **Qiuyan Chen**[*], **Madhu Dikshit**[†], **Yanming Wang**[§], **Carole A. Parent**[‡], and **Matam Vijay-Kumar**[¶,*]

[*]Department of Nutritional Sciences, The Pennsylvania State University, University Park, PA 16802, USA

[†]Pharmacology Division, CSIR-Central Drug Research Institute, Sitapur Road, Lucknow, 226031, India

[‡]Laboratory of Cellular and Molecular Biology, National Cancer Institute, The National Institutes of Health, Bethesda, MD 20892, USA

[§]Center for Eukaryotic Gene Regulation, Department of Biochemistry and Molecular Biology, Pennsylvania State University, University Park, PA 16802, USA

[¶]Department of Medicine, The Pennsylvania State University Medical Center, Hershey, PA 17033, USA

Abstract

Neutrophils are the primary immune cells that respond to inflammation and combat microbial transgression. In order to thrive, the bacteria residing in their mammalian host have to withstand the anti-bactericidal responses of neutrophils. We report that enterobactin (Ent), a catecholate siderophore expressed by *E. coli*, inhibited PMA-induced generation of reactive oxygen species (ROS) and neutrophil extracellular traps (NETs) in both mouse and human neutrophils. Ent also impaired the degranulation of primary granules, inhibited phagocytosis and bactericidal activity of neutrophils, but without affecting their migration and chemotaxis. Molecular analysis revealed that Ent can chelate intracellular labile iron that is required for neutrophil oxidative responses. Other siderophores (pyoverdine, ferrichrome, deferoxamine) likewise inhibited ROS and NETs in neutrophils, thus indicating that the chelation of iron may largely explain their inhibitory effects. To counter iron theft by Ent, neutrophils rely on the siderophore-binding protein lipocalin 2 (Lcn2) in a ‘tug-of-war’ for iron. The inhibition of neutrophil ROS and NETs by Ent was augmented in Lcn2-deficient neutrophils when compared to WT neutrophils, but rescued by the exogenous addition of recombinant Lcn2. Taken together, our findings illustrate the novel concept that microbial siderophore’s iron scavenging property may serve as an anti-radical defense system, that neutralizes immune functions of neutrophils.

[*]**Corresponding Author:** Matam Vijay-Kumar (Vijay), PhD, Department of Nutritional Sciences, The Pennsylvania State University, 222 Chandlee Laboratory, University Park, PA 16802, Off Ph: 814-867-3537, FAX: 814-863-6103, mvk13@psu.edu.
[‖]These authors contributed equally

Disclosures:
The authors have no financial conflicts of interest.

Keywords

Enterochelin; Iron chelation; Reactive Oxygen Species; NETs; Catalytic iron; Lipocalin 2; Siderocalin

Introduction

As the vanguard of the innate immune system, the neutrophils are specialized to combat microbial transgression via the generation of reactive oxygen species (ROS), phagocytosis or degranulation of antimicrobial mediators including myeloperoxidase (MPO) and lipocalin 2 (Lcn2). Moreover, neutrophils can release its DNA to form web-like neutrophil extracellular traps (NETs) to entrap and promote the killing of invading pathogens (1). The immune pressure exerted by neutrophils curtails the growth of many bacteria, yet the Gram-negative *Enterobacteriaceae* could bloom and thrive in the inflamed gut despite the intense inflammatory milieu. Archetypal members of the *Enterobacteriaceae* family, such as *Escherichia coli* and *Salmonella enterica* spp., are capable of exploiting the host-derived nitrate, reactive nitrogen species and ROS to support their anaerobic respiration and growth during inflammation (2–6). However, the mechanisms that allow these bacteria to neutralize the antimicrobial activity of neutrophils are not well understood.

Iron is an essential nutrient for almost all aerobic organisms, yet its participation in redox reactions could aggravate oxidative stress. Accordingly, the host induces the hypoferremia or ‘anemia of inflammation’ as an acute phase response to sequester the labile iron pool (LIP; alias catalytic/reactive iron) (7). This scarcity of iron evokes *E. coli* and *Salmonella* to increase their production of enterobactin (Ent), a prototypical catecholate-type siderophore (Greek: ‘iron carrier’), to acquire iron from the host. The host responds by eliciting the siderophore-binding protein Lcn2 (alias siderocalin or neutrophil gelatinase-associated lipocalin or NGAL) to sequester Ent (8, 9). Such ‘tug-of-war’ between Lcn2 and Ent for iron represents one of the most well-characterized host-pathogen interactions that are highly conserved in humans and other mammals (8).

In this study, we report that Ent can inhibit neutrophil ROS generation, NETs formation, degranulation, and phagocytosis, but without affecting neutrophil polarization and chemotaxis. Our molecular analysis revealed that Ent exerts its immunoregulatory effects by chelating the intracellular iron and LIP in neutrophils. The capacity of Ent to impact neutrophil function was notably augmented in Lcn2-deficient neutrophils when compared to WT neutrophils but rescued by the addition of exogenous Lcn2. Taken together, our findings illustrate the novel concept that Ent may serve as the microbial anti-radical, which confers a survival advantage to bacteria against neutrophils.

Materials and Methods

Reagents

Iron-free Ent (*E. coli*), pyoverdine (*Pseudomonas fluorescens*), ferrichrome (*Ustilago sphaerogena*), deferoxamine mesylate salt, 2,3 dihydroxybenzoic acid (2,3-DHBA), PMA, LPS (*E. coli* 0128: B12), Ca^{+2} ionophore (A23187), DMSO, ferric chloride, PIPES,

Histopaque®-1077 and 1119, RPMI, LB, Dextran, BSA, PFA, Saponin, formyl-Met-Leu-Phe (fMLP) and kanamycin were procured from Sigma (St Louis, MO). Leukotriene B4 (LTB_4) was from Cayman Chemical (Ann Arbor, MI). Carrier-free mouse recombinant Lcn2 (free from endotoxin, siderophore, and iron) was obtained from Cell Signaling (Danvers, MA). Chrome azurol S (CAS) was purchased from Acros Organics (Geel, Belgium).

Mice

*Lcn2*KO mice generated by Dr. Shizuo Akira (Japan) were obtained via Dr. Kelly Smith (University of Washington). MPO-deficient (*Mpo*KO) and NADPH oxidase 2-deficient (*Nox2*KO) mice were procured from Jackson Laboratory (Bar Harbor, ME). *Mpo/Nox2*DKO and peptidyl arginine deiminase-deficient (*Pad4*KO) mice (10) were generated in the PSU animal facility. All the mice are on C57BL/6 (BL6) background and were crossed with BL6 wild-type (WT) mice for more than ten generations.

Ethics Statement

This study was performed in strict accordance with the recommendations in the Guide for the Care and Use of Laboratory Animals of the National Institutes of Health and approved by the Institutional Animal Care and Use Committee (IACUC) at The Pennsylvania State University (IACUC# 43376-1).

Human neutrophil (HL-60) cell line

Human neutrophils (HL-60 cells) were cultured in complete RPMI containing 1.25% DMSO to induce differentiation into neutrophil-like cells as described previously (11).

Isolation of BMDNs and peripheral neutrophils

Bone marrow-derived neutrophils (BMDNs) were isolated from mice (6–8 weeks old; sex-matched) using the Histopaque gradient method (12). This method yielded >95% pure and >99% viable $Ly6G^+$ neutrophils as confirmed by flow cytometry. Blood samples from anonymous human donors were obtained from the NIH Blood Bank research program. Heparinized whole blood from healthy donors was obtained by venipuncture. Human PMNs were isolated from whole blood using dextran sedimentation (3% dextran in 0.9% NaCl) followed by differential centrifugation over Histopaque 1077 as previously described (13, 14). Residual erythrocytes were lysed using hypotonic shock in 0.2% NaCl and neutralization in 1.6% NaCl.

Intracellular ROS assay

Freshly isolated BMDNs/PMNs (2×10^5 cells/well) were pre-incubated with Ent (0, 2.5, 12.5, or 25 μM) or indicated siderophores (2, 3-DHBA, DFO, ferrichrome and pyoverdine; 25 μM) for 30 min before treatment with either PMA (50 nM), LPS (1.0 μg/ml) or calcium ionophore (5.0 μM) for 3 h at 37°C and 5% CO_2. Cells were washed with PBS, stained with 5 μM CellROX® Deep Red dye (Molecular probes) for 30 min at 37°C in the dark and washed twice with PBS. Fluorescence was measured by flow cytometry (Accuri c6, BD Biosciences) and analyzed using the FlowJo software (Becton Dickinson). Intracellular ROS

was expressed as fold change of mean fluorescence intensity (MFI) normalized to the controls.

NETs quantification

SYTOX Green (5.0 μM) was added to the BMDNs/PMNs at the initial stage of PMA stimulation described above. The plates were read in a Spectra MAX Gemini fluorescence microplate reader (Molecular Devices; Sunnyvale, CA) with a filter setting of 485 (excitation)/527 (emission). The data were presented as fold change of NETs formation normalized to the controls (15). To visualize NETs, the BMDNs (5×10^5/wells) were seeded in 8-wells glass-chambered slides (Lab-TekII) in incomplete RPMI media, treated with PMA and Ent as described, and incubated for 3 h at 37°C and 5% CO_2. Cells were fixed with 3.7% formaldehyde for 10 min and stained with anti-mouse H3-Cit mAb (overnight, 4°C, Abcam) and Fluoroshield™ with DAPI (Sigma) for 5 min. Fluorescent microscopic images were acquired using 40x magnification in different fields on Olympus FV10i - LIV confocal microscope.

Bacteria

Non-pathogenic wild-type *E. coli* (EcK12) and its isogenic mutant of *3-dehydroquinate synthase* (ΔaroB) were acquired from The *E. coli* Genetic Stock Center, Yale University. An isogenic mutant of *ferrienterobactin permease* (*ΔfepA*; EcK12), *ΔfepA*/*ΔaroB*-double mutant (EcK12), and GFP-expressing *E. coli* (BL21) were gifts from Dr. Kathleen Postle (The Pennsylvania State University). *E. coli* mutant of *ferric uptake regulator* (*Δfur*; EcK12) was a gift from Dr. James Imlay (University of Illinois).

Stimulation of BMDNs with bacteria

E. coli and its isogenic Ent mutants *(ΔaroB, ΔfepA and Δfur*) were grown overnight in LB media (containing 50 μg/mL kanamycin) at 37°C with shaking (200 rpm). Equal numbers of bacterial CFUs were adjusted based on their optical density at 600 nm, pelleted and resuspended in incomplete RPMI media, and heat-killed at 90°C for 5 min. Heat-killed bacteria were added to PMA-treated BMDNs at MOI of 100:1 and incubated for 3 h at 37°C and 5% CO_2. Intracellular ROS and NETs were analyzed as described above.

Bacteria survival assay

BMDNs and PMNs (2×10^6 cells/well in 1 ml incomplete RPMI media without antibiotic) were plated in 6-wells plate. Ent (25 μM) was added to the respective wells and incubated for 1 h at 37°C and 5% CO_2. Next, cells were infected with *E. coli* at MOI of 50:1 and incubated for 3 h at 37°C and 5% CO_2. At post-infection, culture supernatants were collected, serially-diluted and plated on LB agar plates. The neutrophil fractions were pelleted, washed and resuspended in 1 ml of 50% PBS containing Triton X-100 (0.1%) to release phagocytosed bacteria, and plated on LB agar plates. Plates were incubated overnight at 37°C for CFU counting.

Phagocytosis assay

GFP-expressing *E. coli* (16) were opsonized by incubating equal volumes of heat-inactivated 10% mouse serum and bacterial suspension in PBS for 1 h at 37°C. BMDNs were treated with Ent (25 μM) at 37°C for 30 min. The bacteria, after three washes in PBS, were added to the BMDNs at the bacteria-to-neutrophils ratio of 50:1 and incubated at 37°C for 2 h. Cells were fixed with ice-cold 1% formaldehyde in PBS and washed twice with PBS to remove extracellular bacteria. The percentage of the phagocytosed bacteria was determined by BD LSR-Fortessa flow cytometry and analyzed using FlowJo software.

Chrome azurol S (CAS) assay

CAS agar plates and CAS liquid reagent were prepared as described previously (17). Equal CFUs of isogenic *E. coli* Ent mutants were spotted on CAS agar plate, incubated overnight at 37°C, and monitored for the formation of orange halo. CAS remains blue in color when complexed with iron, but turns orange when iron is chelated by other iron chelators. To estimate Ent released by bacteria, the culture supernatants (diluted 4X in 100 μl) were added to the CAS liquid reagent (100 μl), incubated at room temperature for 20 min, and the change in absorbance was read at 630 nm. Results were estimated using a standard curve generated from iron-free Ent.

ELISA

MPO and Lcn2 protein levels in the BMDNs culture supernatant and cell lysates (prepared in RIPA buffer containing 1x protease inhibitor cocktail) were analyzed using Duoset ELISA kits from R&D Systems (Minneapolis, MN) according to manufacturer instructions.

Lactate dehydrogenase assay

Lactate dehydrogenase (LDH) levels in the BMDNs culture supernatant were measured using the kit from Randox (Crumlin, UK) according to the manufacturer's instructions.

Immunoblotting

BMDNs cell lysates were subjected to Western blot using standard procedure and probed with antibodies to citrullinated histone 3 (H3-Cit; a marker for NETs), total H3, and PAD4 (Abcam).

Neutrophil apoptosis

BMDNs viability and apoptosis were measured using the FITC Annexin-V apoptosis detection kit (BD Biosciences) according to manufacturer's instruction. Results were analyzed using LSR-Fortessa flow cytometry and FlowJo software and presented as the percentage of early (Annexin-V positive) and late apoptotic (Annexin-V and propidium iodide positive) cells.

Neutrophil polarization analysis

1% BSA coated 8-well chambered coverglass slides (Lab-Tek, Thermo Fisher Scientific) were used. PMNs (2.5×10^5 cells/well) were incubated with vehicle (DMSO) or treated with Ent (100 μM) for 2 h at 37°C. Post-Ent treatment, neutrophils were stimulated for 5 min at

37°C with either fMLP (10 nM) or LTB_4 (100 nM). Non-adherent cells were washed away and the remaining adherent cells were fixed with 4% PFA for 10 min. Cells were later permeabilized using 0.05% Saponin containing PBS, blocked and stained for F-Actin and nucleus using Rhodamine-Phalloidin and DAPI (Molecular Probes, Thermo Fisher Scientific). Fluorescence microscopy of samples was performed using a 40x objective lens on a Zeiss observer microscope (Zeiss Axiovert S100 microscope). Multiple fields were acquired for each condition and a minimum of 100 cells was analyzed for each experiment. PMNs displaying enriched F-Actin at the protrusive front were considered polarized and the percentage of such polarized cells in each condition was visually quantified.

Chemotaxis analysis using under-agarose assay

1% BSA coated 6-well plates (In Vitro Scientific, California) were used. The assay was performed as previously described (13). Briefly, 0.5% SeaKem ME agarose (Lonza) in 50% each of PBS and RPMI without phenol red was allowed to solidify in wells. Three 1 mm diameter wells were carved out at 2 mm distance between each other. Vehicle (DMSO) or Ent treated (100 μM for 2 h at 37°C) cells were stained with CellTracker Red CMPTX dye according to manufacturer's protocol (Life Technologies, Thermo Fisher Scientific). Cells were washed and re-suspended in RPMI without phenol red and 10 μl (5×10^4 cells) of vehicle or Ent-treated cells were added to the extreme wells and were allowed to migrate towards the center well containing 10 μl of either fMLP (100 nM) or LTB_4 (250 nM). Fluorescence microscopy of samples was performed using a 1x objective lens (Zeiss Axiovert S100 microscope) and images of the same field of view were acquired every 45 seconds for a total period of 60 min. Image sequences from under-agarose movies were used to track 20 or more cells per condition in each experiment. Each image sequence was loaded on Image J and cells were followed using the Manual Tracking plugin. The output files containing the × and y coordinates were then used to measure the accumulated distance and directionality using the Chemotaxis plugin available for Image J.

Intracellular labile iron assay

BMDNs were incubated for 15 min at 37°C and 5% CO_2 with 0.5 μM Calcein acetoxymethyl ester (Sigma). The cells were washed twice and treated with Ent or DFO (25 μM) for 2 h. Following washing with PBS, cells were analyzed by LSR-Fortessa flow cytometer, and the MFI was calculated using the FlowJo software. The levels of intracellular labile iron were calculated by subtracting the difference in the MFI (ΔF) before and after treatment with iron chelators (18). Percent chelation was calculated by using the formula: (ΔF/control MFI) × 100.

Bleomycin-detectable labile iron assay

The assay was performed as outlined by Burkitt et al. (19) with modifications described previously (20). In principle, ascorbic acid converts Fe^{+3} into Fe^{+2}, which in combination with bleomycin, causes DNA breaks. Ent or DFO was pre-incubated with Fe^{+3} (0.005–200 μM) for 10 min prior to the addition of the assay mixture (20) and incubated at 37°C for 2 h. Bleomycin/iron-induced damage to DNA corresponds to the loss in the ethidium bromide-enhanced fluorescent signal (excitation 510 nm; emission 590 nm) and presented as the percentage of labile iron.

Statistical analysis

All experiments were performed in triplicate and data presented are representative of three independent experiments. All values in the results are expressed as mean ± SEM. Statistical significance between two groups was analyzed using unpaired, two-tailed t-test. Data from more than two groups was compared using a one-way analysis of variance (ANOVA) followed by Dunnett's post hoc test (when to compare the mean of each column with the mean control column) or Tukey's multiple comparison tests (when to compare the mean of each column with the mean of every other column). $p< 0.05$ was considered as statistically significant and denoted as * $p< 0.05$ and ** $p<0.01$ and *** $p<0.001$. All statistical analyses were performed with the GraphPad Prism 7.0 program (GraphPad, Inc, La Jolla, CA).

Results

Enterobactin inhibits neutrophil ROS generation

Neutrophils are one of the professional immune cells that mediate bacterial killing during infection. Our recent finding that *E. coli*-derived Ent potently inhibits the activity of purified MPO from human neutrophils (21) raises the prospect that Ent may also modulate other neutrophil functions. To advance toward this hypothesis, we isolated BMDNs from BL6 mice and treated the cells with Ent. While we observed a substantial level of intracellular ROS in the BMDNs, the treatment with Ent inhibited their ROS generation in a dose and time-dependent manner (Fig. 1A, 1B). We repeated the experiments using BMDNs stimulated with PMA, which activates NADPH oxidase and upregulates their ROS generation. Ent likewise mitigated PMA-induced ROS generation in BMDNs in a dose and time-dependent manner (Fig. 1C, 1D, 1E). Moreover, Ent was effective in inhibiting the generation of ROS in BMDNs activated by an array of potent neutrophil stimulators, including LPS and Ca^{+2} ionophore (Fig. 1F). Similar results were observed when experiments were repeated using human neutrophil-like cell line (nHL-60) and human PMNs (Fig. 1G, 1H, 1I).

To assess the extent of Ent-mediated inhibition on ROS generation, we next measured the levels of ROS in Ent-treated WT BMDNs in comparison to the BMDNs deficient in NADPH oxidase 2 (NOX2) and MPO as negative controls. As anticipated, the genetic loss of NOX2 (22, 23) abrogated the capacity of BMDNs to upregulate ROS in response to PMA stimulation (Fig. 1J). Presumably due to having an intact NOX2, the MPO-deficient BMDNs could still generate ROS to some extent in response to PMA, but this was abrogated upon treatment with Ent (Fig. 1J). Intriguingly, the loss of detectable ROS in Ent-treated WT and MPO-deficient BMDNs were comparable to MPO/NOX2 double-deficient BMDNs that are ROS-deficient (Fig 1J); such outcome further affirms the efficacy of Ent in inhibiting the generation of ROS in neutrophils.

To rule out whether Ent-mediated inhibition of neutrophil ROS is due to increased cell death, we assessed the markers of early and late apoptosis in Ent-treated BMDNs. The percentage of apoptotic cells, however, were comparable between Ent- and vehicle-treated BMDNs (Fig. 1K), thus indicating that Ent-mediated effects are not due to altered cell viability. Next, we assayed the cell-free supernatant for lactate dehydrogenase (LDH), whose

release indicates cytosolic leakage and cell death (24). The reduced LDH release from Ent + PMA-treated BMDNs affirms the efficacy of Ent in inhibiting neutrophil activation, in comparison to PMA-treated BMDNs (Fig. 1L).

Enterobactin inhibits NETs formation and degranulation

Since ROS are indispensable for the production of NETs (25), we envisioned that Ent-mediated inhibition of ROS generation may impede the formation of NETs as well. Indeed, we observed 1.7 to 2-fold reduction in the release of NETs from Ent + PMA-treated BMDNs, compared with BMDNs treated with PMA alone (Fig. 2A, 2B). The inhibition of NETs generation by Ent correlates with the decrease in the levels of NETs markers (H3-Cit and PAD4 (26) in Ent + PMA-treated BMDNs compared with PMA-treated controls (Fig. 2C). Quantification of extracellular DNA with SYTOX green indicates that WT BMDNs could generate NETs even at the basal level, when compared to the NETs-deficient BMDNs isolated from *Pad4*KO mice (10, 27) as negative control (Fig. 2D). Such basal NETs in WT BMDNs, however, was prevented upon treatment with Ent (Fig. 2E, 2F). The formation of NETs increased substantially upon stimulation with PMA, yet Ent was effective in inhibiting PMA-induced NETs in a dose and time-dependent manner (Fig. 2G, 2H). Similar inhibition of NETs formation by Ent was observed when experiments were repeated with LPS or Ca^{+2} ionophore treated BMDNs (Fig. 2I), and PMA-treated human PMNs (Fig. 2J, 2K) and nHL-60 cell line (Fig. 2L).

To investigate whether Ent could inhibit neutrophil degranulation, we assayed the cell-free supernatants from BMDNs for granular markers such as MPO and Lcn2, which correlates with the release of primary and secondary granules, respectively (28, 29). The addition of Ent to control and PMA-treated BMDNs blocked the release of their primary granules as indicated by the reduced levels of MPO in the supernatant (Fig. 2M). However, Ent did not impair the capacity of BMDNs to degranulate their secondary granules or Lcn2 in response to PMA (Fig. 2N), thus suggesting the specificity of Ent in inhibiting the release of primary, but not secondary granules.

We next evaluated the effect of Ent on the acquisition of neutrophil polarity and chemotaxis. Human PMNs were stimulated with sub-saturating concentrations of two independent and potent chemoattractants, fMLP, and LTB_4. We found that pre-treatment with Ent, even at 100 μM, had little or no impact on the ability of PMNs to polarize in response to fMLP or LTB_4 (Supplemental Fig. 1A, 1B). Furthermore, Ent-treated PMNs exhibited a chemotactic response to both fMLP and LTB_4 that was comparable to vehicle-treated PMNs. Indeed, the total distance migrated and directionality of migration was unchanged by Ent treatment (Supplemental Fig. 1C, 1D, 1E). These findings establish that Ent has no significant impact on the ability of PMNs to polarize and chemotaxis to fMLP and LTB_4.

Ent protects bacteria against the anti-bactericidal activity of neutrophils

To address whether Ent-producing bacteria can inhibit neutrophil ROS and NETs, we took advantage *E. coli* isogenic mutants that are deficient in Ent (Δ*aroB*) or overexpress Ent (Δ*fepA* and Δ*fur*). We first determined that Δ*fepA* and Δ*fur* mutants produced more Ent than WT *E.coli* based on the extent of halo formation on the CAS agar plate. By using the more

sensitive CAS liquid assay, we noted that Δ*fur* secreted a higher amount of Ent into the culture supernatant followed by Δ*fepA*, WT and Δ*aroB* strains (Fig. 3B). The discrepancy in the levels of siderophores detected on CAS agar (Δ*fepA* > Δ*fur*) and CAS liquid (Δ*fur* > Δ*fepA*) are likely to be due to technical difference (e.g., growth conditions) of the assays, but are nevertheless sufficient to establish that Δ*fepA* and Δ*fur* produced more Ent than WT and Δ*aroB* strains. Although the bacteria themselves induce NETs formation, we observed that their level of Ent production was inversely correlated with their capacity to inhibit the basal ROS production from the BMDNs (Fig. 3C, 3D). When the PMA-stimulated BMDNs were treated with heat-killed Ent mutant bacteria, their ROS and NETs responses were inhibited in the order of Δ*fur* > Δ*fepA* > WT > Δ*aroB*, which correlates with the levels of Ent production in these strains (Fig. 3E, 3F, 3G). The bacterial culture supernatants, which contains Ent, were also effective in inhibiting PMA-induced ROS and NETs from BMDNs in the order of Δ*fur* > Δ*fepA* > WT > Δ*aroB* (Fig. 3H, 3I). Our observations that WT *E. coli* and isogenic mutants were not as effective as their culture supernatant in inhibiting the BMDNs PMA-induced ROS could be explained by the possibility that Ent may have accumulated more in the culture supernatant. However, the unanticipated reduction in PMA-induced ROS by Δ*aroB* supernatant suggests the possibility that there are other unknown bacterial metabolites which may also play a role in alleviating the oxidative responses.

The inhibition of neutrophil ROS and NETs responses by Ent may confer a survival advantage to Ent-producing bacteria. Consistent with this notion, we observed that the BMDNs treated with exogenous Ent were impaired in mediating the killing of WT *E. coli*; viable bacteria recovered from Ent-treated BMDNs were ~7.3-fold higher in the assay supernatant and ~4-fold higher in the lysed-neutrophil fraction, compared with the bacteria recovered from vehicle-treated BMDNs (Fig. 4A). Similar results were also observed in human PMNs (Fig. 4B). To assess whether endogenously-produced Ent also offers similar protection, we next examined the survivability of Δ*fepA* and Δ*fepA*/Δ*aroB E. coli* mutant against the BMDNs. The Ent-overexpressing Δ*fepA* mutant was substantially protected from the bactericidal activity of BMDNs compared with the Ent-deficient Δ*fepA*/Δ*aroB* mutant, which survived poorly (Fig. 4C). Besides promoting the survivability of extracellular and phagocytosed bacteria, Ent also inhibited the capacity of BMDNs to phagocytose bacteria by approximately 1.3-fold, in comparison to vehicle-treated control (Fig. 4D, 4E).

Ent-mediated inhibition of neutrophil ROS and NETs is counter-regulated by Lcn2

Given that Ent did not impair the release of Lcn2 from neutrophils, we thus envisioned that the secreted Lcn2 may be able to neutralize the effects of Ent. While Ent inhibited PMA-induced ROS by 1.8-fold in WT BMDNs, relative to PMA-only control, the extent of inhibition increased to 3.6-fold in Lcn2-deficient BMDNs (Fig. 5A). Furthermore, Ent inhibited PMA-induced NETs by 2.4-fold in WT BMDNs and 4.3-fold in Lcn2-deficient BMDNs, when compared with their corresponding PMA-only treated BMDNs (Fig. 5B). These observations suggest that Ent nearly twice as effective in inhibiting ROS and NETs in Lcn2-deficient neutrophils than WT neutrophils. Since Lcn2 is known to bind Ent in a stoichiometry ratio of 1:1, we thus investigated whether adding rLcn2 to Ent in such ratio would protect Lcn2-deficient neutrophils from being inhibited. Treatment with exogenous

rLcn2 indeed rescued Lcn2-deficient neutrophils from Ent and restored their capacity to generate basal and PMA-induced ROS and NETs (Fig. 5C, 5D, 5E, 5F).

Ent inhibits neutrophil functions by chelating cytosolic labile iron

The intricate interaction between Lcn2 and Ent reported herein is highly evocative of their 'tug-of-war' for iron; which compelled us to investigate whether alteration in cellular iron may provide the mechanistic explanation on how ROS and NETs are regulated by Lcn2 and Ent. By using the cytochemical calcein-AM method (30–32), we demonstrate that Lcn2-deficient BMDNs contain approximately two-fold more cytosolic LIP compared with WT BMDNs (Fig. 6A); such result could potentially explain our observations that Lcn2-deficient BMDNs generated more PMA-induced ROS than WT BMDNs (Fig. 5A).

The LIP assay employed herein requires the addition of DFO to chelate iron from calcein, thus allowing the detection of displaced calcein as a measurement of cellular LIP (30–32). Based on this principle, we envision that the calcein-AM assay can be modified to mechanistically examine the effects of Ent on BMDNs, i.e., by employing Ent as the iron chelator instead of DFO. The use of Ent in the modified assay yielded higher MFI readings compared to DFO (Fig. 6B); the higher sensitivity with Ent may be due to its superior affinity and kinetics in chelating iron than DFO that is known to be slow iron chelator (33). Although the level of cytosolic LIP in Lcn2-deficient BMDNs was still detected as two-fold higher than WT BMDNs in this modified assay, our use of Ent provided several key mechanistic insights. First, the readout itself indicates that Ent can permeate the neutrophil membrane and remain intact in the cytosolic compartment. Second, the readout also implicates that Ent retains its iron-chelating property and potently chelates the cytosolic LIP in the neutrophils. The majority of neutrophil oxidative responses requires LIP (34), thus its reduced bioavailability due to chelation by Ent could be a potential mechanism by which Ent hijacks neutrophil functions.

To ascertain whether Ent could quench the reactivity of LIP, we modified the bleomycin-based LIP detection assay that was originally developed to quantify LIP in biological samples (19). In our modified assay system, we instead prepared a series of samples with known concentrations of labile iron and tested whether Ent could quench their detection. Intriguingly, 50 μM of Ent completely prevented the detection of labile iron ranging between 0.005 to 50 μM, but not when the concentration of labile iron exceeds 50 μM (Fig. 6C). Such finding coincides with the well-accepted notion that Ent binds iron in a stoichiometry ratio of 1:1 (35); it also affirms that Ent can effectively quench the reactivity of bound-iron, but not the excess unbound iron.

To address whether chelation of labile iron could be the underlying mechanism of Ent-mediated inhibition of neutrophil functions, we next tested other siderophores for their ability to inhibit PMA-induced ROS and NETs in BMDNs. Weak iron chelator such as 2,3-dihydroxybenzoic acid (2,3-DHBA; a monomeric Ent) modestly mitigated PMA-induced neutrophil ROS and NETs (Fig. 6D, 6E). Other iron chelators such as ferrichrome (fungal siderophore from *U. sphaerogena*), bacterial siderophores pyoverdine (from *P. fluorescens*) and DFO (from *Streptomyces pilosus*) mitigated PMA-induced ROS and NETs to a greater extent (Fig. 6D, 6E). However, our data suggests that Ent mediated a superior inhibition in

the order of Ent > pyoverdine > DFO > ferrichrome (Fig. 6D, 6E), which is consistent with the property of Ent having an unmatched affinity (K_d of 10^{-49}M) for iron (36).

The chelation of LIP by Ent may impede neutrophil ROS responses that are dependent on labile iron. To test whether Lcn2 could prevent Ent from chelating cytosolic LIP, we next performed the modified calcein-AM assay using Ent and rLcn2. The addition of Ent modestly increased the MFI reading in WT BMDNs (indicating that Ent was chelating iron from the intracellular calcein-iron complex), but the increase was more pronounced in Lcn2-deficient BMDNs (Fig. 6F). The addition of rLcn2 remarkably suppresses the MFI reading of the elevated labile iron in Lcn2-deficient BMDNs to the levels that are comparable to WT BMDNs (Fig. 6F).

Discussion

The iron acquisition system of *E. coli* encodes the enzymes for the synthesis of Ent, the archetype siderophore for Gram-negative bacteria. The production of Ent, however, is metabolically expensive given the number of enzymes involved to generate Ent from its aromatic amino acid precursors (37). Accordingly, it was presumed that Ent may exert a plethora of key physiological functions that could account for its high metabolic cost (38), aside from acquiring iron to support bacterial growth. Such notion has been demonstrated in studies whereby Ent was shown to be fundamental for *E. coli* to establish colonization in the mammalian gut (39), develop mature biofilms (40, 41), alleviate oxidative stress (42, 43), and neutralize the anti-microbial activity of MPO (21). The multifaceted property of Ent is further exemplified by our findings that it could inhibit an array of neutrophil functions, including ROS generation, NETs formation, degranulation, phagocytosis and bacterial killing activity. Besides conferring a survival advantage to *E. coli*, the Ent-mediated inhibition of mucosal ROS generation may also be of advantage to other gut commensals in achieving a stable colonization (44). Such notion is exemplified by the intricate Ent-dependent crosstalk between microbial community (41, 45, 46) and the fact that various non-Ent-producing bacteria have, nonetheless, evolved to express the receptor for Ent (47).

Various biological processes depend upon the reactivity of labile iron, a redox engine to catalyze chemical reactions that are essential to life. The oxidative responses of neutrophils are particularly iron-dependent (48), in addition to the fact that many of their pro-inflammatory mediators (i.e., MPO, NADPH oxidase and iNOS) are heme proteins. Investigating how Ent hijacks neutrophil activity revealed that the hydrophobic Ent could permeate cellular membranes and chelate the cytosolic labile iron (free/catalytic iron) of neutrophils. Our observations that other siderophores (i.e., pyoverdine, ferrichrome, DFO) likewise inhibited neutrophil ROS and NETs further implicate that the chelation of iron may explain their inhibitory effects. The inhibition of NETs formation by siderophores is rather unprecedented and may allude to the possible requirement of labile iron during the formation of NETs. Analogous to the ability of *Streptococcus sp.* to escape NETs by expressing DNases (49, 50), the production of siderophore by *E. coli* and other bacteria may be a key mechanism that allows them to evade NETs-mediated killing. We considered that the loss of NETs response may be secondary to the inhibition of ROS production or MPO (21) by Ent, in light of the contention that NETs response requires the activity of NADPH

oxidase and MPO (22, 23, 25, 51). Nevertheless, further studies are needed to investigate whether Ent could directly modulate NETs formation.

The inhibitory effects of Ent on neutrophils can be counter-regulated by Lcn2 that sequesters bacterial siderophores with a high affinity (K_d of 0.41 nM) (35). Lcn2 is expressed by a variety of immune and non-immune cells, although the neutrophils are the richest source of Lcn2 (52). While Lcn2 is regarded as the primary defense against the iron theft by Ent (35), our group have previously reported that Lcn2 also preserve the activity of MPO from being inhibited by Ent (21). In the current study, we further highlight the importance of Lcn2 in shielding the neutrophils and their functions from being compromised by Ent. The 'tug-of-war' between Lcn2 and Ent, however, may exert selective immune pressure on *E. coli* to evolve or acquire the ability to produce Lcn2-resistant or stealth siderophores (e.g., pyoverdine) (53). In such regard, the inability of Lcn2 to neutralize the stealth siderophores may potentially compromise neutrophil functions from effectively mediate the clearance of pathogens (54).

The bacterial siderophore from *Streptomyces pilosus*, DFO, has been widely used clinically to treat patients with iron overload and hereditary haemochromatosis. However, the use of DFO can potentially promote bacterial and fungal infection (55–57); such side effects are postulated to be due to the delivery of iron-bound DFO to the pathogens (58). Our findings suggest that the siderophore-induced loss of neutrophil activity could also potentially promote a state of 'functional neutropenia', thus exacerbating the susceptibility to infection. The development of iron chelators without the side effects of inhibiting neutrophil functions could be further explored in future studies in optimizing siderophore-based therapy in treating iron-related disorders.

There may be circumstances in which neutrophil inactivation would be desirable, as in the case of inflammatory disorders whereby dysregulated neutrophils could incur collateral damage to bystander tissues. Such possibility is implicated by the clinical use of the probiotic *E. coli* Nissle 1917 (EcN) to treat gut inflammation (59), whose efficacy in preventing the colonization of enteropathogens is purported to be due to their unique capacity to express four types of siderophores (i.e., Ent, aerobactin, yersiniabactin and salmochelin) (60). While EcN has been reported to exhibit anti-inflammatory properties, their siderophore production may, in part, explain its ability to immuno-regulate host inflammatory responses. The property of siderophore in quenching the redox potential of labile iron may also safeguard both host and bacteria from the iron-induced generation of free radicals via Fenton reaction. The emerging concept that bacterial siderophores are not merely iron chelators, but are also immunoregulatory metabolites, could certainly be investigated in future studies for their therapeutic potential in treating inflammatory diseases.

Supplementary Material

Refer to Web version on PubMed Central for supplementary material.

Acknowledgments

We thank Dr. A. Catharine Ross and Dr. Na Xiong for their critical input. We thank and dedicate this study to our long-standing collaborator Dr. Niels Borregaard for his helpful discussion and support for this study.

Funding: This work was supported by a grant from the National Institutes of Health R01 (DK097865) to MV-K. VS is supported by CCFA′s Research Fellowship Award.

Abbreviations

BMDNs	Bone Marrow Derived Neutrophils
PMNs	Peripheral Neutrophils
Ent	Enterobactin
ROS	Reactive oxygen species
NETs	Neutrophil extracellular traps

References

1. Brinkmann V, Reichard U, Goosmann C, Fauler B, Uhlemann Y, Weiss DS, Weinrauch Y, Zychlinsky A. Neutrophil extracellular traps kill bacteria. Science. 2004; 303:1532–1535. [PubMed: 15001782]
2. Rivera-Chavez F, Winter SE, Lopez CA, Xavier MN, Winter MG, Nuccio SP, Russell JM, Laughlin RC, Lawhon SD, Sterzenbach T, Bevins CL, Tsolis RM, Harshey R, Adams LG, Baumler AJ. Salmonella uses energy taxis to benefit from intestinal inflammation. PLoS pathogens. 2013; 9:e1003267. [PubMed: 23637594]
3. Spees AM, Wangdi T, Lopez CA, Kingsbury DD, Xavier M, Winter SE, Tsolis RM, Baumler AJ. Streptomycin-induced inflammation enhances Escherichia coli gut colonization through nitrate respiration. mBio. 2013; 4
4. Winter SE, Lopez CA, Baumler AJ. The dynamics of gut-associated microbial communities during inflammation. EMBO reports. 2013; 14:319–327. [PubMed: 23478337]
5. Winter SE, Winter MG, Xavier MN, Thiennimitr P, Poon V, Keestra AM, Laughlin RC, Gomez G, Wu J, Lawhon SD, Popova IE, Parikh SJ, Adams LG, Tsolis RM, Stewart VJ, Baumler AJ. Host-derived nitrate boosts growth of E. coli in the inflamed gut. Science. 2013; 339:708–711. [PubMed: 23393266]
6. Lopez CA, Winter SE, Rivera-Chavez F, Xavier M, Poon V, Nuccio SP, Tsolis RM, Baumler AJ. Phage-mediated acquisition of a type III secreted effector protein boosts growth of salmonella by nitrate respiration. mBi. 2012; 3
7. Nemeth E, Rivera S, Gabayan V, Keller C, Taudorf S, Pedersen BK, Ganz T. IL-6 mediates hypoferremia of inflammation by inducing the synthesis of the iron regulatory hormone hepcidin. The Journal of clinical investigation. 2004; 113:1271–1276. [PubMed: 15124018]
8. Chakraborty S, Kaur S, Guha S, Batra SK. The multifaceted roles of neutrophil gelatinase associated lipocalin (NGAL) in inflammation and cancer. Biochimica et biophysica acta. 2012; 1826:129–169. [PubMed: 22513004]
9. Martensson J, Xu S, Bell M, Martling CR, Venge P. Immunoassays distinguishing between HNL/NGAL released in urine from kidney epithelial cells and neutrophils. Clinica chimica acta; international journal of clinical chemistry. 2012; 413:1661–1667. [PubMed: 22609864]
10. Li P, Li M, Lindberg MR, Kennett MJ, Xiong N, Wang Y. PAD4 is essential for antibacterial innate immunity mediated by neutrophil extracellular traps. The Journal of experimental medicine. 2010; 207:1853–1862. [PubMed: 20733033]
11. Arroyo A, Modriansky M, Serinkan FB, Bello RI, Matsura T, Jiang J, Tyurin VA, Tyurina YY, Fadeel B, Kagan VE. NADPH oxidase-dependent oxidation and externalization of

phosphatidylserine during apoptosis in Me2SO-differentiated HL-60 cells. Role in phagocytic clearance. The Journal of biological chemistry. 2002; 277:49965–49975. [PubMed: 12376550]

12. Swamydas M, Lionakis MS. Isolation, purification and labeling of mouse bone marrow neutrophils for functional studies and adoptive transfer experiments. Journal of visualized experiments: JoVE. 2013:e50586. [PubMed: 23892876]
13. Majumdar R, Tavakoli Tameh A, Parent CA. Exosomes Mediate LTB4 Release during Neutrophil Chemotaxis. PLoS biology. 2016; 14:e1002336. [PubMed: 26741884]
14. Afonso PV, Janka-Junttila M, Lee YJ, McCann CP, Oliver CM, Aamer KA, Losert W, Cicerone MT, Parent CA. LTB4 is a signal-relay molecule during neutrophil chemotaxis. Developmental cell. 2012; 22:1079–1091. [PubMed: 22542839]
15. Gupta AK, Giaglis S, Hasler P, Hahn S. Efficient neutrophil extracellular trap induction requires mobilization of both intracellular and extracellular calcium pools and is modulated by cyclosporine A. PloS one. 2014; 9:e97088. [PubMed: 24819773]
16. Lee SK, Keasling JD. A propionate-inducible expression system for enteric bacteria. Applied and environmental microbiology. 2005; 71:6856–6862. [PubMed: 16269719]
17. Schwyn B, Neilands JB. Universal chemical assay for the detection and determination of siderophores. Analytical biochemistry. 1987; 160:47–56. [PubMed: 2952030]
18. Prus E, Fibach E. Flow cytometry measurement of the labile iron pool in human hematopoietic cells. Cytometry Part A: the journal of the International Society for Analytical Cytology. 2008; 73:22–27. [PubMed: 18044720]
19. Burkitt MJ, Milne L, Raafat A. A simple, highly sensitive and improved method for the measurement of bleomycin-detectable iron: the ‘catalytic iron index’ and its value in the assessment of iron status in haemochromatosis. Clinical science. 2001; 100:239–247. [PubMed: 11222109]
20. Yeoh BS, Aguilera Olvera R, Singh V, Xiao X, Kennett MJ, Joe B, Lambert JD, Vijay-Kumar M. Epigallocatechin-3-Gallate Inhibition of Myeloperoxidase and Its Counter-Regulation by Dietary Iron and Lipocalin 2 in Murine Model of Gut Inflammation. The American journal of pathology. 2016; 186:912–926. [PubMed: 26968114]
21. Singh V, Yeoh BS, Xiao X, Kumar M, Bachman M, Borregaard N, Joe B, Vijay-Kumar M. Interplay between enterobactin, myeloperoxidase and lipocalin 2 regulates E. coli survival in the inflamed gut. Nature communications. 2015; 6:7113.
22. Fuchs TA, Abed U, Goosmann C, Hurwitz R, Schulze I, Wahn V, Weinrauch Y, Brinkmann V, Zychlinsky A. Novel cell death program leads to neutrophil extracellular traps. The Journal of cell biology. 2007; 176:231–241. [PubMed: 17210947]
23. Parker H, Dragunow M, Hampton MB, Kettle AJ, Winterbourn CC. Requirements for NADPH oxidase and myeloperoxidase in neutrophil extracellular trap formation differ depending on the stimulus. Journal of leukocyte biology. 2012; 92:841–849. [PubMed: 22802447]
24. Chan FK, Moriwaki K, De Rosa MJ. Detection of necrosis by release of lactate dehydrogenase activity. Methods in molecular biology. 2013; 979:65–70. [PubMed: 23397389]
25. Kirchner T, Moller S, Klinger M, Solbach W, Laskay T, Behnen M. The impact of various reactive oxygen species on the formation of neutrophil extracellular traps. Mediators of inflammation. 2012; 2012:849136. [PubMed: 22481865]
26. Wang Y, Li M, Stadler S, Correll S, Li P, Wang D, Hayama R, Leonelli L, Han H, Grigoryev SA, Allis CD, Coonrod SA. Histone hypercitrullination mediates chromatin decondensation and neutrophil extracellular trap formation. The Journal of cell biology. 2009; 184:205–213. [PubMed: 19153223]
27. Wang Y, Wysocka J, Sayegh J, Lee YH, Perlin JR, Leonelli L, Sonbuchner LS, McDonald CH, Cook RG, Dou Y, Roeder RG, Clarke S, Stallcup MR, Allis CD, Coonrod SA. Human PAD4 regulates histone arginine methylation levels via demethylimination. Science. 2004; 306:279–283. [PubMed: 15345777]
28. Liu Y, Merlin D, Burst SL, Pochet M, Madara JL, Parkos CA. The role of CD47 in neutrophil transmigration. Increased rate of migration correlates with increased cell surface expression of CD47. The Journal of biological chemistry. 2001; 276:40156–40166. [PubMed: 11479293]

29. Faurschou M, Borregaard N. Neutrophil granules and secretory vesicles in inflammation. Microbes and infection. 2003; 5:1317–1327. [PubMed: 14613775]
30. Cabantchik ZI, Glickstein H, Milgram P, Breuer W. A fluorescence assay for assessing chelation of intracellular iron in a membrane model system and in mammalian cells. Analytical biochemistry. 1996; 233:221–227. [PubMed: 8789722]
31. Esposito BP, Epsztejn S, Breuer W, Cabantchik ZI. A review of fluorescence methods for assessing labile iron in cells and biological fluids. Analytical biochemistry. 2002; 304:1–18. [PubMed: 11969183]
32. Glickstein H, El RB, Shvartsman M, Cabantchik ZI. Intracellular labile iron pools as direct targets of iron chelators: a fluorescence study of chelator action in living cells. Blood. 2005; 106:3242–3250. [PubMed: 16020512]
33. Xiao X, Yeoh BS, Saha P, Tian Y, Singh V, Patterson AD, Vijay-Kumar M. Modulation of urinary siderophores by the diet, gut microbiota and inflammation in mice. The Journal of nutritional biochemistry. 2016; 41:25–33. [PubMed: 27951517]
34. Kakhlon O, Cabantchik ZI. The labile iron pool: characterization, measurement, and participation in cellular processes(1). Free radical biology & medicine. 2002; 33:1037–1046. [PubMed: 12374615]
35. Goetz DH, Holmes MA, Borregaard N, Bluhm ME, Raymond KN, Strong RK. The neutrophil lipocalin NGAL is a bacteriostatic agent that interferes with siderophore-mediated iron acquisition. Molecular cell. 2002; 10:1033–1043. [PubMed: 12453412]
36. Loomis LD, Raymond KN. Solution Equilibria of Enterobactin and Metal Enterobactin Complexes. Inorg Chem. 1991; 30:906–911.
37. Raymond KN, Dertz EA, Kim SS. Enterobactin: an archetype for microbial iron transport. Proceedings of the National Academy of Sciences of the United States of America. 2003; 100:3584–3588. [PubMed: 12655062]
38. Lv H, Hung CS, Henderson JP. Metabolomic analysis of siderophore cheater mutants reveals metabolic costs of expression in uropathogenic Escherichia coli. Journal of proteome research. 2014; 13:1397–1404. [PubMed: 24476533]
39. Pi H, Jones SA, Mercer LE, Meador JP, Caughron JE, Jordan L, Newton SM, Conway T, Klebba PE. Role of catecholate siderophores in gram-negative bacterial colonization of the mouse gut. PloS one. 2012; 7:e50020. [PubMed: 23209633]
40. May T, Okabe S. Enterobactin is required for biofilm development in reduced-genome Escherichia coli. Environmental microbiology. 2011; 13:3149–3162. [PubMed: 21980953]
41. Keogh D, Tay WH, Ho YY, Dale JL, Chen S, Umashankar S, Williams RB, Chen SL, Dunny GM, Kline KA. Enterococcal Metabolite Cues Facilitate Interspecies Niche Modulation and Polymicrobial Infection. Cell host & microbe. 2016; 20:493–503. [PubMed: 27736645]
42. Peralta DR, Adler C, Corbalan NS, Paz Garcia EC, Pomares MF, Vincent PA. Enterobactin as Part of the Oxidative Stress Response Repertoire. PloS one. 2016; 11:e0157799. [PubMed: 27310257]
43. Adler C, Corbalan NS, Peralta DR, Pomares MF, de Cristobal RE, Vincent PA. The alternative role of enterobactin as an oxidative stress protector allows Escherichia coli colony development. PloS one. 2014; 9:e84734. [PubMed: 24392154]
44. Knaus UG, Hertzberger R, Pircalabioru GG, Yousefi SP, Branco Dos Santos F. Pathogen control at the intestinal mucosa - H2O2 to the rescue. Gut microbes. 2017; 0
45. Griffin AS, West SA, Buckling A. Cooperation and competition in pathogenic bacteria. Nature. 2004; 430:1024–1027. [PubMed: 15329720]
46. Thulasiraman P, Newton SM, Xu J, Raymond KN, Mai C, Hall A, Montague MA, Klebba PE. Selectivity of ferric enterobactin binding and cooperativity of transport in gram-negative bacteria. Journal of bacteriology. 1998; 180:6689–6696. [PubMed: 9852016]
47. Rutz JM, Abdullah T, Singh SP, Kalve VI, Klebba PE. Evolution of the ferric enterobactin receptor in gram-negative bacteria. Journal of bacteriology. 1991; 173:5964–5974. [PubMed: 1717434]
48. Murakawa H, Bland CE, Willis WT, Dallman PR. Iron deficiency and neutrophil function: different rates of correction of the depressions in oxidative burst and myeloperoxidase activity after iron treatment. Blood. 1987; 69:1464–1468. [PubMed: 3032307]

49. Buchanan JT, Simpson AJ, Aziz RK, Liu GY, Kristian SA, Kotb M, Feramisco J, Nizet V. DNase expression allows the pathogen group A Streptococcus to escape killing in neutrophil extracellular traps. Current biology: CB. 2006; 16:396–400. [PubMed: 16488874]
50. Beiter K, Wartha F, Albiger B, Normark S, Zychlinsky A, Henriques-Normark B. An endonuclease allows Streptococcus pneumoniae to escape from neutrophil extracellular traps. Current biology: CB. 2006; 16:401–407. [PubMed: 16488875]
51. Metzler KD, Fuchs TA, Nauseef WM, Reumaux D, Roesler J, Schulze I, Wahn V, Papayannopoulos V, Zychlinsky A. Myeloperoxidase is required for neutrophil extracellular trap formation: implications for innate immunity. Blood. 2011; 117:953–959. [PubMed: 20974672]
52. Borregaard N, Cowland JB. Neutrophil gelatinase-associated lipocalin, a siderophore-binding eukaryotic protein. Biometals: an international journal on the role of metal ions in biology, biochemistry, and medicine. 2006; 19:211–215.
53. Fischbach MA, Lin H, Zhou L, Yu Y, Abergel RJ, Liu DR, Raymond KN, Wanner BL, Strong RK, Walsh CT, Aderem A, Smith KD. The pathogen-associated iroA gene cluster mediates bacterial evasion of lipocalin 2. Proceedings of the National Academy of Sciences of the United States of America. 2006; 103:16502–16507. [PubMed: 17060628]
54. Su Q, Guan T, He Y, Lv H. Siderophore Biosynthesis Governs the Virulence of Uropathogenic Escherichia coli by Coordinately Modulating the Differential Metabolism. Journal of proteome research. 2016; 15:1323–1332. [PubMed: 26954697]
55. Windus DW, Stokes TJ, Julian BA, Fenves AZ. Fatal Rhizopus infections in hemodialysis patients receiving deferoxamine. Annals of internal medicine. 1987; 107:678–680. [PubMed: 3662280]
56. Boelaert JR, de Locht M, Van Cutsem J, Kerrels V, Cantinieaux B, Verdonck A, Van Landuyt HW, Schneider YJ. Mucormycosis during deferoxamine therapy is a siderophore-mediated infection. In vitro and in vivo animal studies. The Journal of clinical investigation. 1993; 91:1979–1986. [PubMed: 8486769]
57. Schubert S, Autenrieth IB. Conjugation of hydroxyethyl starch to desferrioxamine (DFO) modulates the dual role of DFO in Yersinia enterocolitica infection. Clinical and diagnostic laboratory immunology. 2000; 7:457–462. [PubMed: 10799461]
58. Kontoghiorghes GJ, Kolnagou A, Skiada A, Petrikkos G. The role of iron and chelators on infections in iron overload and non iron loaded conditions: prospects for the design of new antimicrobial therapies. Hemoglobin. 2010; 34:227–239. [PubMed: 20524813]
59. Scaldaferri F, Gerardi V, Mangiola F, Lopetuso LR, Pizzoferrato M, Petito V, Papa A, Stojanovic J, Poscia A, Cammarota G, Gasbarrini A. Role and mechanisms of action of Escherichia coli Nissle 1917 in the maintenance of remission in ulcerative colitis patients: An update. World journal of gastroenterology. 2016; 22:5505–5511. [PubMed: 27350728]
60. Deriu E, Liu JZ, Pezeshki M, Edwards RA, Ochoa RJ, Contreras H, Libby SJ, Fang FC, Raffatellu M. Probiotic bacteria reduce salmonella typhimurium intestinal colonization by competing for iron. Cell host & microbe. 2013; 14:26–37. [PubMed: 23870311]

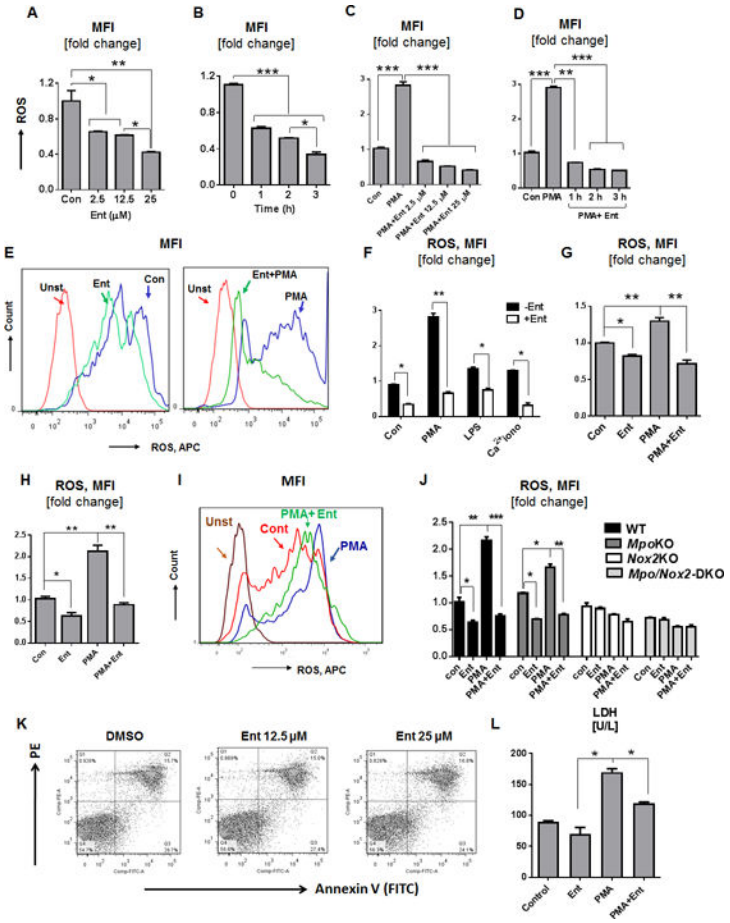

Figure 1. Ent inhibits neutrophil ROS generation

BMDNs from WT mice were treated with Ent and measured for their generation of intracellular ROS as described in the *Materials and Methods*. (**A** and **B**) Bar graphs denote the Ent dose and time-dependent effects on basal ROS generation, and (**C** and **D**) Ent dose and - time-dependent effects on PMA-stimulated ROS generation. (**E**) Histograms represent the flow cytometric analysis of basal (left) and PMA-induced (right) ROS generation, quantified as MFI. (**F**) Bar graphs showing the influence of Ent on LPS and Ca^{+2} ionophore treated BMDNs on ROS generation. (**G**) Human neutrophil-like cell line (nHL-60) were treated with Ent and monitored for ROS generation. (**H**) Human peripheral neutrophils were isolated and the effects of Ent were evaluated ROS generation in human neutrophils. (**I**) Histograms represent the flow cytometric analysis of ROS generation in MFI. (**J**) BMDNs were isolated from WT, *Mpo*KO, *Nox2*KO, and *Mpo*/*Nox2*DKO mice and effects of Ent on ROS generation was determined. (**K**) Effects of Ent on BMDNs apoptosis were measured by flow cytometry using the Annexin-V/PI positivity. Dot plots showing the % of early and late apoptosis in Ent-treated BMDNs. (**L**) Bar graphs represent the released lactate dehydrogenase (LDH) in the culture supernatant. MFI= Mean fluorescence intensity. *In vitro* assays were performed in triplicates and are representative of two independent mouse experiments. Results are expressed as mean ± SEM. * $p < 0.05$, ** $p<0.01$, and *** $p<0.001$.

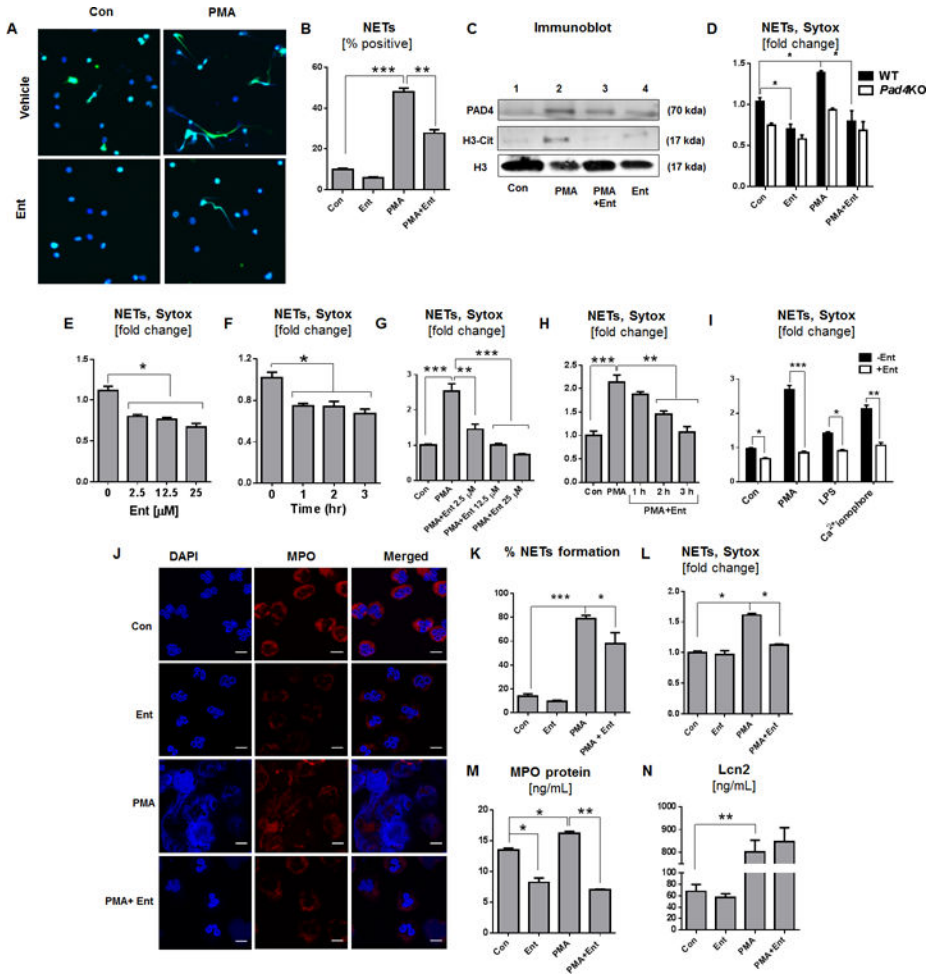

Figure 2. Ent prevents the NETs formation and degranulation in Neutrophil

BMDNs from WT mice were treated with Ent and the formation of NETs was visualized. (**A**) Representative images of NETs visualized by co-staining of citrullinated histone (H3-Cit, green) and DNA (DAPI, blue). Original magnification 60x. (**B**) Semi-quantitative image analysis of % NETs formation. (**C**) Immunoblot for PAD4, H3-Cit, total histone (H3) in the neutrophil cell lysate. Histone 3 (H3) used as a loading control. BMDNs were treated with Ent and the formation of NETs was quantified by the SYTOX Green-based fluorimetric method. (**D**) BMDNs were isolated from WT and *Pad4*KO mice and effects of Ent on NETs was determined. (**E** and **F**) Effect of Ent on basal NETs formation in a - time and - dose-dependent manner. (**G** and **H**) Bar graphs designate the Ent dose and time-dependent effects on PMA-induced NETs formation (fold change) (**I**) Influence of Ent on LPS and Ca^{+2} ionophore treated BMDNs on NETs formation. The effects of Ent on human peripheral neutrophils were evaluated on NETs formation. (**J**) NETs are visualized by co-staining of MPO (red) and DNA (DAPI, blue). Original magnification 60x. (**K**) Bar graphs represent % NETs formation. (**L**) Neutrophil-like HL-60 cells were treated with Ent and monitored for NETs formation. (**M** and **N**) Degranulation of neutrophil was assessed by quantifying the levels of MPO and Lcn2 in the culture supernatant. MFI= Mean fluorescence intensity. *In*

vitro assays were performed in triplicates and are representative of two independent mouse experiments. Results are expressed as mean ± SEM. * $p < 0.05$, ** $p < 0.01$, and *** $p < 0.001$.

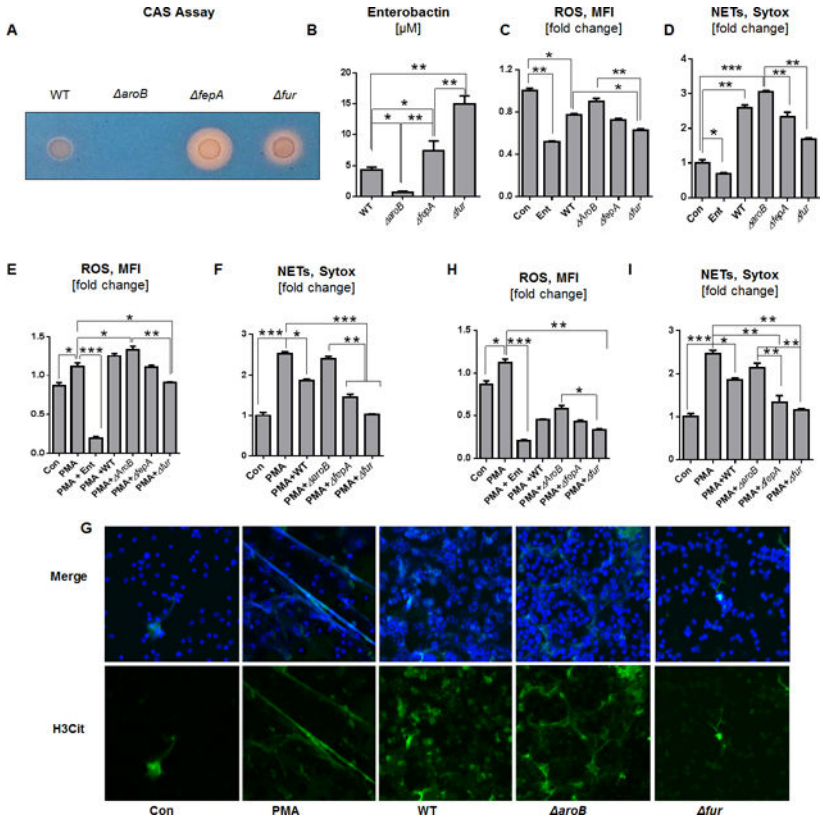

Figure 3. Ent impedes the antimicrobial effects of neutrophils

Production of Ent by *E. coli* and their isogenic mutants (WT, Δ*aroB*, Δ*fepA*, and Δ*fur*) were assessed using CAS assays. (**A**) The formation of orange halo indicates Ent production by *E. coli* mutant on CAS plate. (**B**) Bar graphs indicate the detection of Ent in the bacterial culture supernatant via CAS liquid assay. (**C** and **D**) BMDNs were treated with WT or Ent mutant bacteria (MOI of 100:1) and measured for ROS and NETs generation. (**E** and **F**) PMA-stimulated BMDNs were treated with heat-killed WT or Ent mutant bacteria and measured for ROS and NETs generation. (**G**) Representative images of NETs co-stained with H3-Cit (green) and DNA (DAPI, blue). Original magnification 60x. (**H** and **I**) Bar graphs represent the effects of bacterial culture supernatants on PMA-induced ROS and NETs formation in BMDNs. *In vitro* assays were performed in triplicates and are representative of two independent mouse experiments. Results are expressed as mean ± SEM. * $p < 0.05$, ** $p < 0.01$, and *** $p < 0.001$.

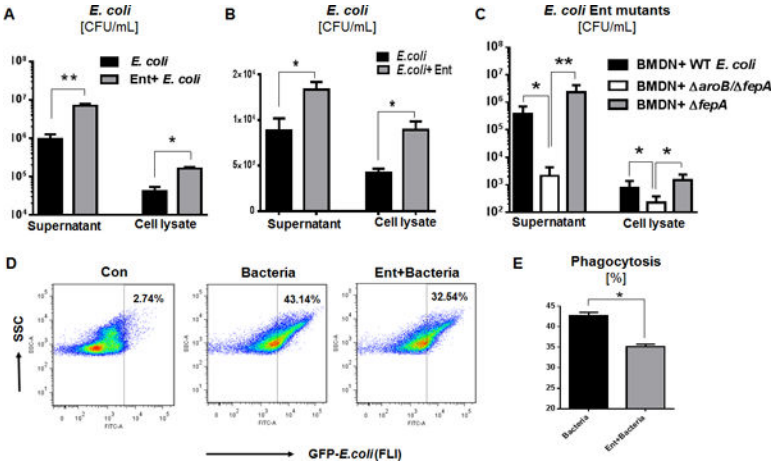

Figure 4. Ent protects against neutrophil-mediated bacterial killing

(**A**) Neutrophil-mediated bacteria killing assay in presence of exogenous Ent (25 μM) with WT *E. coli*. (**B**) PMNs-mediated bacteria killing assay in presence of exogenous Ent (25 μM) with WT *E. coli*. (**C**) WT *E. coli* and its isogenic mutants employed in the killing assay to assess the effect of endogenously-derived Ent. (**D** and **E**) Phagocytosis (%) was determined by flow cytometric analysis of opsonized GFP-expressing *E. coli* by neutrophils. *In vitro* assays were performed in triplicates and are representative of two independent mouse experiments. Results are expressed as mean ± SEM. * $p < 0.05$, ** $p<0.01$, and *** $p<0.001$.

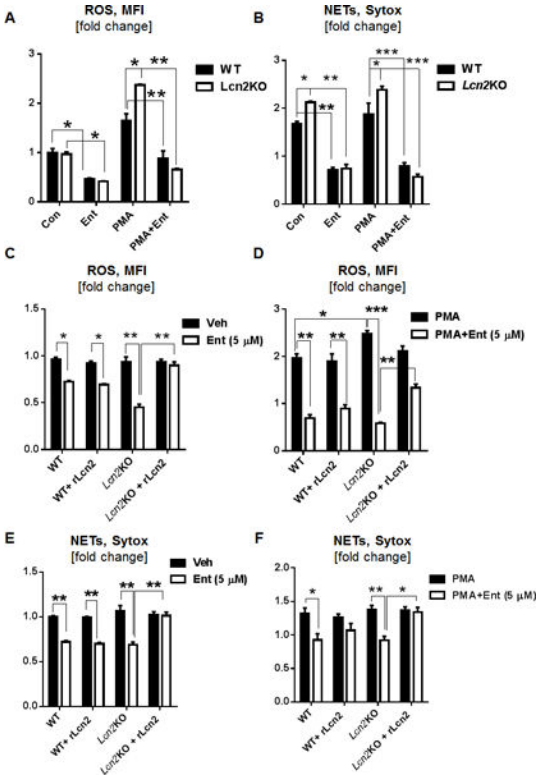

Figure 5. rLcn2 dampens the inhibitory effects of Ent and reinstates the capacity of neutrophils to generate ROS and NETs

(**A**, **B**) BMDNs from *Lcn2*KO and WT mice were treated with PMA and Ent and quantitated for their generation of ROS and NETs. (**C-F**) Exogenous rLcn2 was added to PMA and Ent treated WT and *Lcn2*KO BMDNs and analyzed for their generation of (**C**) basal ROS, (**D**) PMA-induced ROS, (**E**) basal NETs, and (**F**) PMA-induced NETs. *In vitro* assays were performed in triplicates and are representative of two independent mouse experiments. Results are expressed as mean ± SEM. * $p < 0.05$, ** $p<0.01$, and *** $p<0.001$.

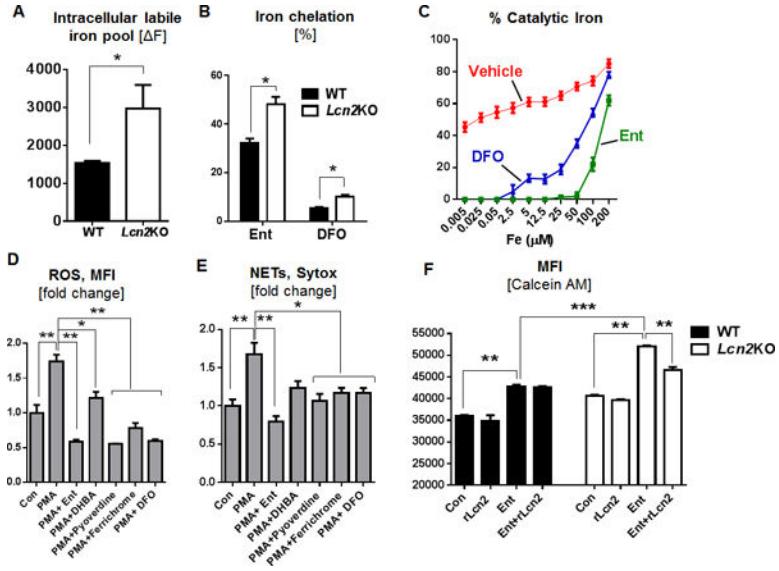

Figure 6. Ent chelates cytosolic labile iron pool (LIP) in neutrophils and mitigates their anti-microbial functions

BMDNs from *Lcn2*KO mice and their WT littermates were incubated with Ent. (**A**) Cytosolic LIP was quantitated using the Calcein-AM based flow cytometry method. (**B**) Bar graphs represent the % intracellular iron chelation by Ent and DFO in *Lcn2*KO and in WT neutrophils. (**C**) Line graphs showing the effects of Ent and DFO in quenching the bleomycin-based LIP detection assay. Influence of other microbial siderophores on the basal and PMA-induced (**D**) ROS generation and (**E**) NETs formation in WT BMDNs. (**F**) Bar graphs represent the intracellular LIP by Calcein-AM assay using Ent and rLcn2 in Lcn2-deficient and WT BMDNs. MFI= Mean fluorescence intensity. In vitro assays were performed in triplicates and are representative of two independent mouse experiments. Results are expressed as mean ± SEM. * $p < 0.05$, ** $p < 0.01$, and *** $p < 0.001$.